Hindawi
Advances in Materials Science and Engineering
Volume 2021, Article ID 8186851, 13 pages
https://doi.org/10.1155/2021/8186851

Research Article

Research on Preparation and Performance of Clay-Based Shield Tunnel Nonsintered Bricks

Sibin Chen,[1] Hao Jiang,[2] Huitang Xing,[1] Jing Wang ,[2] Yongliang Huang,[1] Guangbin Wei,[2] Yijie Zhang ,[2] and Dongshuai Hou[3]

[1]*Jinan Rail Transit Group Co.,Ltd., Jinan, Shandong 250101, China*
[2]*Qilu Transportation College of Shandong University, Jinan, Shandong 250061, China*
[3]*Qingdao University of Technology, Qingdao, Shandong 266520, China*

Correspondence should be addressed to Jing Wang; wjingsdu@163.com and Yijie Zhang; jjzyjie@126.com

Received 31 August 2021; Revised 26 September 2021; Accepted 26 October 2021; Published 16 December 2021

Academic Editor: Shengwen Tang

With the rapid development of rail transit in China, the number and scale of underground engineering construction have increased significantly, and a large amount of shield muck has been generated, which has brought great challenges to the urban environment. The reuse of shield muck has become an important research direction in underground engineering construction. In this paper, a nonsintered brick is prepared with shield muck soil as the matrix. The influence of different doping amounts of lime, fly ash, cement, and polyvinyl alcohol on porosity, density, water absorption, saturation coefficient, compressive strength, and other properties was explored to realize the resource utilization of shield dregs and at the same time obtain excellent performance nonsintered bricks. Through research, it is found that when the lime doping amount is 10% and the cement doping amount is 5%, with the increase of the fly ash doping amount, the overall compressive strength increases significantly, and the maximum compressive strength can reach 13.69 MPa. Although the doping of trace amounts of polyvinyl alcohol reduces the compressive strength, it can significantly reduce the compressive strength and mass loss rate after 15 freeze-thaw cycles.

1. Introduction

The rail transit construction of China is developing rapidly, and shield machines have been widely used as the main equipment for rail transit construction. At present, the amount of Shield muck in my country is more than 119 million tons per year, but the actual resource utilization rate is less than 1%. The traditional methods of open-air stacking or landfilling are mainly used for treatment, which not only invades the land and pollutes the soil and groundwater, but also slags. In the process of soil transportation, it pollutes roads and destroys the appearance of the city. Shield muck has become the most major urban construction waste, which has brought great challenges to the urban environment [1–3].

In recent years, many scholars have successively begun to study the reuse technology of shield muck, which has significantly improved the application value of shield muck. Shield muck can be used as building materials to prepare building materials including synchronous grouting materials, high-performance ceramsites, and functional bricks (permeable bricks, pavement bricks, and sintered bricks) [4–26]. In terms of synchronous grouting research, Qian et al. [9] carried out a proportioning test by a uniform test method and performed linear regression and single-factor analysis on the test results. It is found that all parameters of the prepared synchronous grouting material meet the requirements, which provides a basis for the feasibility of preparing the synchronous grouting material from the shield muck. At the same time, Cui and Tan [10] studied high-performance synchronous grouting materials prepared with clay. High-performance synchronous grouting material was studied by taking red clay as an example, modified by epoxy resin. In terms of high-performance ceramsite research, Zhang et al. [11–13] studied the effects of fly ash, sludge, and straw on the density grade of muck ceramsite. According to

the optimization of raw material formula and process parameters, the muck ceramsite with a density grade of 700–900 was fabricated, and their macroscopic performance and microstructure were analyzed. Liu et al. [14–16] processed a novel method for preparing ultra-lightweight ceramsite with fly ash. A ceramsite with bulk density of 340 kg/m, particle density of 0.68 g/cm^3, and cylinder compressive strength of 1.02 MPa were obtained. In the research of functional bricks [17–26], relevant scholars used river mud, industrial manganese slag, foundation pit slag, and engineering slag as aggregates, supplemented by inorganic cementing materials, such as cement and fly ash, and successfully prepared nonburning powder mud bricks, nonburning manganese slag bricks, and nonburning clay brick. It indirectly proves that the slag can be used as nonsintered brick aggregate, but there are still major limitations, and more theoretical support and experimental research are needed. Gencel et al. [27] studied the recycling of industrial slags in the production of fired clay bricks. In summary, although the shield tunnel muck has been studied in grouting materials and high-performance ceramsite, it is more advantageous to prepare functional bricks from shield tunnel muck in terms of utilization rate and utilization effect. At present, most of the researches on the preparation of functional bricks from shield muck are focused on adding a small amount of muck, which fails to well stimulate the activity of silico-alumina minerals in the slag. At the same time, organic doping can improve the overall performance of the material. Therefore, this article researched nonsintered bricks with shield muck as the matrix, inorganic cementing materials as auxiliary materials, and trace organic doping.

2. Preparation Test and Test Method

2.1. Raw Material. Shield muck comes from Jinan shield tunnel muck. After the sample is crushed by a jaw crusher, it is passed through a 32-mesh sieve to ensure that the particle size of the sample material is less than 0.5 mm. The XRD diagram of the shield muck is shown in Figure 1. The lime is quicklime, which is produced by Zhucheng Yangchun Cement Co., Ltd., with a CaO content of 87% and a fineness of 320 m^2/kg. The lime slurry formed after quicklime slaked can significantly improve workability. The cement is produced by Zhucheng Yangchun Cement Co., Ltd., and its performance indicators meet the requirements of GB 175–1999 and GB/T 2542–2012 [28]. "Portland Cement, Ordinary Portland Cement." Fly ash: the nonfired bricks mainly exist as cementing components and microaggregate components. Polyvinyl alcohol is analytically pure and has a molecular weight of 20000. The chemical composition of the main raw materials is shown in Table 1.

2.2. Test Plan. This test explores the influence of the ratio of waste soil to lime, cement, fly ash, and polyvinyl alcohol (15% water-to-binder ratio) on density, water absorption, saturation coefficient, porosity, microstructure, and mechanical properties. The test plan is shown in Table 2.

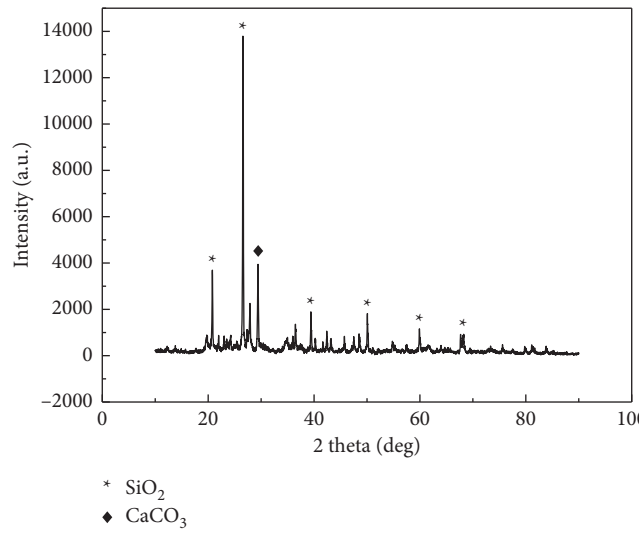

Figure 1: XRD diagram of shield muck.

2.3. Preparation of Nonfired Bricks. After the shield muck is crushed by a jaw crusher, it is passed through a 32-mesh standard sieve. The powder is dried in a drying box at 100°C for 2 hours and then naturally cooled to room temperature. According to the test plan, weigh the shield dregs, lime, cement, fly ash, and polyvinyl alcohol and mix them evenly (water-binder ratio 15%). A 30 t hydraulic press was used to press and shape the abovementioned uniformly mixed raw materials in a 50 mm mold with a molding pressure of 10 MPa. The resulting slag brick sample size was a cube of 50 mm × 50 mm × 50 mm. The obtained sample was sealed with a plastic film, then placed in the curing room, and cured for 28 days under standard conditions [temperature (20 ± 2) °C and relative humidity 90%–95%, to obtain the corresponding sample. Related test equipment and test samples are shown in Figure 2.

2.4. Characterization Method of Nonfired Brick. Density, water absorption, and saturation coefficient are tested following GB/T 2542—2012 "Test Method for Wall Bricks"; TDR-10 automatic freezing-thawing box produced by Zhongke Company was used in freeze-thaw cycles. The microstructure characterization method uses the AXS D8 X-ray diffractometer of German Bruker Company to perform XRD phase analysis on the nonfired bricks. JSM-6490LV scanning electron microscope (SEM) of Japan JEOL company is used to characterize the morphology, structure, morphology, and distribution of nonfired bricks. The mechanical performance characterization method adopts the MTS electronic universal testing machine to test the compressive strength and mechanical properties of the nonfired brick samples. The porosity test uses the nuclear magnetic resonance nanoporosity analyzer NMRC12-010V produced by Suzhou Newmai Co., Ltd. to reduce the test error and ensure the repeatability of the test. Each test was carried out three times.

Table 1: Chemical composition of main raw materials (%).

Name	Loss on ignition	SiO_2	Al_2O_3	Fe_2O_3	CaO	MgO	R_2O	SO_3	Total
Shield muck	10.4	53.4	13.5	6.4	10.0	1.8	4.5	—	100
Cement	1.76	21.8	5.5	3.81	61.85	1.69	1.05	2.54	100
Fly ash	8.1	50.6	28.4	6.1	3.8	1.1	1.9	—	100

Table 2: Experimental program.

Serial number	Muck (%)	Lime (%)	Cement (%)	Fly ash (%)	Polyvinyl alcohol (%)
Test 1	80	20	0	0	0
Test 2	70	30	0	0	0
Test 3	60	40	0	0	0
Test 4	50	50	0	0	0
Test 5	60	30	0	10	0
Test 6	50	30	0	20	0
Test 7	40	30	0	30	0
Test 8	30	30	0	40	0
Test 9	65	30	5	0	0
Test 10	60	30	10	0	0
Test 11	55	30	15	0	0
Test 12	50	30	20	0	0
Test 13	60	10	5	25	0
Test 14	55	10	5	30	0
Test 15	50	10	5	35	0
Test 16	45	10	5	40	0
Test 17	45	10	5	40	0.5
Test 18	45	10	5	40	0.75
Test 19	45	10	5	40	1
Test 20	45	10	5	40	1.25

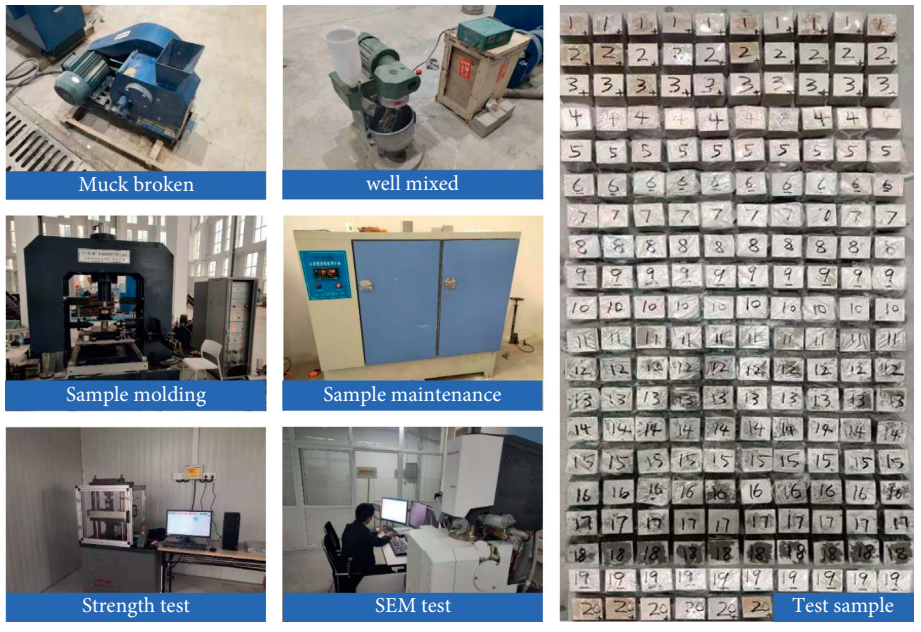

Figure 2: Related test equipment and test samples.

3. Results and Analysis

3.1. Mechanical Properties. Figure 3(a) shows the influence of different contents of lime, fly ash, and cement on tensile strength. From the figure, the compressive strength decreases with the increase of lime content. When the lime content is 40%, the compressive strength reaches the lowest value of 3.19 MPa and then increases. The reason is that when the lime content increases, the reaction releases a lot of heat and generates more $CaCO_3$, which causes volume expansion, resulting in a large number of pores, even microcracks, and the strength decreases. When the lime

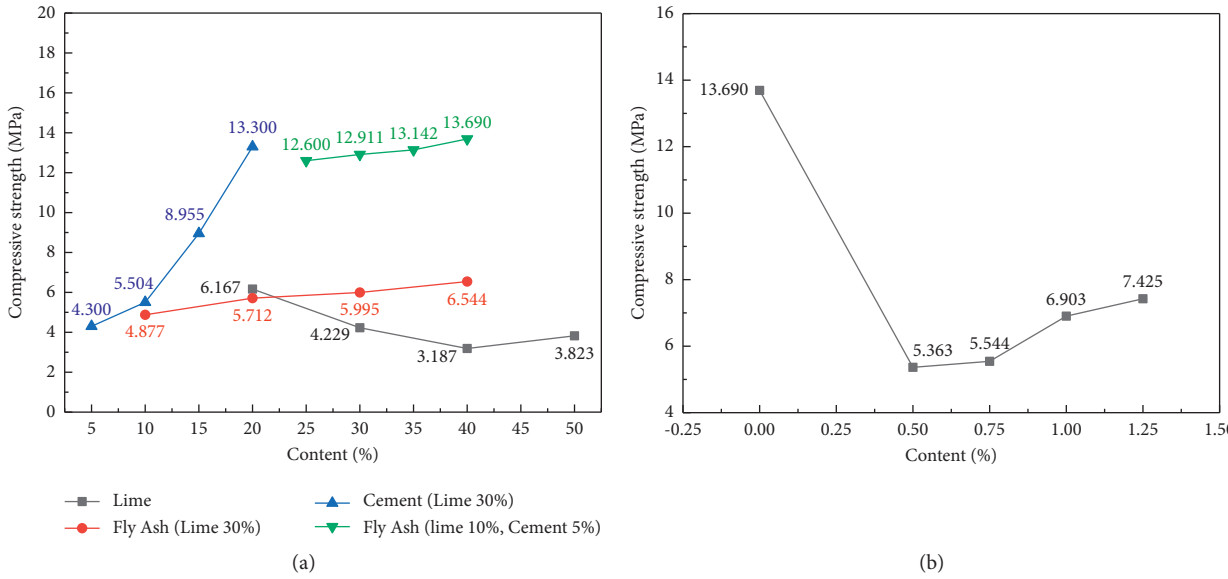

Figure 3: The influence of lime, fly ash, cement (a), and polyvinyl alcohol (muck 45%, lime 10%, cement 5%, and fly ash 40%) (b) on tensile strength.

content reaches 40%, the volume expansion and microcracks cause the strength to decrease. The factor tends to be flat; with the continuous increase of $CaCO_3$, the compressive strength has increased, and there is influence of fly ash content on compressive strength (lime 30%); when the lime content is 30%, with the increase of fly ash content, the compressive strength shows an upward trend, and the fly ash content is 40%; the compressive strength reaches the maximum value of 6.54 MPa, but the lime content is too high, resulting in lower overall compressive strength; there was an effect of cement content on the compressive strength (lime 30%). With the increase of cement content, the compressive strength gradually increases, and the maximum compressive strength is 13.3 MPa. The reason is that the high activity of cement will promote the hydration reaction of C2S and C3S and generate a large number of hydrated silicate (C-S-H) gels, thereby improving the strength, and a large amount of hydrate silicate (C-S-H) gel is formed to form high strength. On the other hand, the hydrated $Ca(OH)_2$ generates hydraulic cementitious materials to increase strength. The increase in compressive strength value is more obvious. There is influence of fly ash content on strength; when the lime content is 10% and the cement content is 5%, as the proportion of fly ash increases, the compressive strength gradually increases, and the maximum value reaches 13.69 MPa. The reason is that due to the glass bead effect of fly ash, the glass beaded fly ash can make the slag particles easier to accumulate and compact under pressure. At the same time, the fly ash has higher activity and is easy to interact with shield slag. Hydration generates C-S-H gel to improve compressive strength. As shown in Figure 3(b), the content of polyvinyl alcohol can significantly reduce the compressive strength. When the content of polyvinyl alcohol is 0.5%, the compressive strength reaches the lowest value of 5.36 MPa. The compressive strength gradually increases with the increase of the amount of quicklime. The reason is that the quicklime reaction releases a large amount of heat so that a small amount of polyvinyl alcohol is carbonized and exists in the collective, reducing the density, and the porosity increases significantly, which promotes the decrease of the strength. The remaining part of the polyvinyl alcohol has a binding effect, and the compressive strength is slightly increased.

3.2. Water Absorption and Saturation Coefficient. Water absorption and saturation coefficient are important performance indicators that reflect the stability and durability of nonburning slag bricks. Figure 4(a) shows the influence of lime content on water absorption; with the increase of lime content, the water absorption of samples immersed in room temperature water for 24 hours and boiled for 3 hours gradually increases. With the increase of lime content, the porosity increases and the water absorption rate gradually increases. In addition, CaO has strong hygroscopicity. With the increase of CaO, the water absorption of the sample increases. As shown in Figure 4(b), with the increase of the fly ash content, the water absorption of the samples immersed in room temperature water for 24 hours and the samples boiled for 3 hours gradually decreased. As shown in Figure 4(c), with the increase of cement content, the water absorption of samples immersed in room temperature water for 24 h and samples boiled for 3 h gradually decreased. The reason is that the particle size of the slag particles is smaller and the specific surface area is larger, resulting in strong water absorption of the muck. In addition, with the increase of muck, the proportion of hydrated gel products decreases, and the porosity increases, resulting in greater water absorption. Figure 4(d) shows the influence of fly ash content on water absorption. As the proportion of fly ash increases, the water absorption of samples immersed in room temperature water for 24 hours and samples boiled for 3 hours

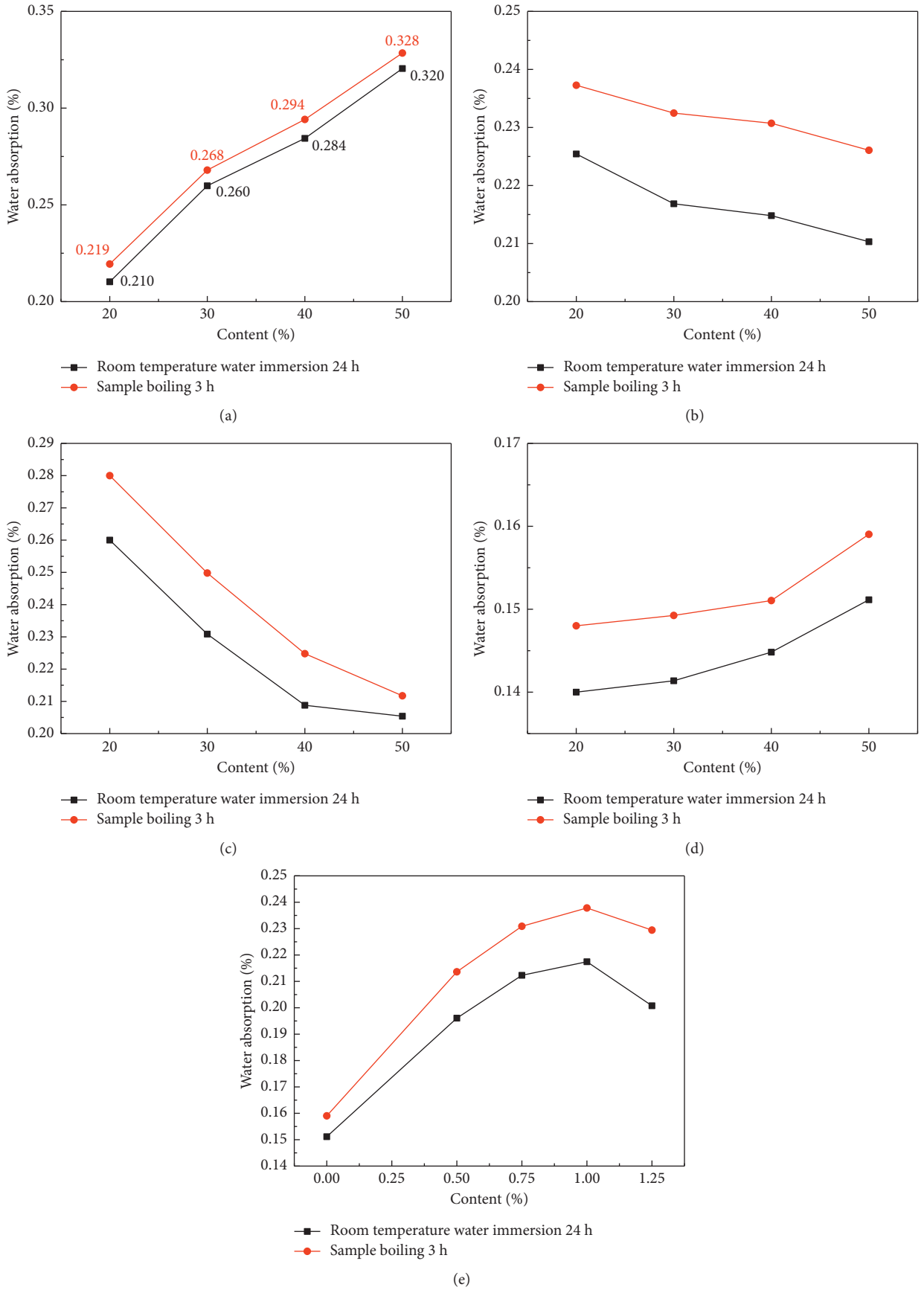

Figure 4: The influence of lime, fly ash (lime 30%), cement (lime 30%), fly ash (lime 10%, cement 5%), and polyvinyl alcohol (lime 10%, cement 5%, and fly ash 40%) dosage on water absorption.

gradually increases. When the lime content is 10% and the cement content is 5%, the porosity is small, and the increase in fly ash content has little effect on its porosity. Fly ash has a microaggregate effect, is spherical, has a large specific surface area, and has strong water absorption. Therefore, with the increase of fly ash, the water absorption rate of the sample gradually increases. Figure 4(e) shows the influence of polyvinyl alcohol dosage on water absorption. The content of polyvinyl alcohol can significantly increase the water absorption rate of samples immersed in room temperature water for 24 h and boiling for 3 h. With the increase of the content, the water absorption rate of samples immersed in room temperature water for 24 h and boiling for 3 h first increases and then decreases. Because the addition of polyacrylic alcohol forms a hydrophobic layer, but the content is less, the hydrophobic effect is less than the influence of porosity and specific surface area on the water absorption rate. It shows an increase in water absorption. When the polyvinyl alcohol content reaches 1%, the increase in porosity has less influence on the water absorption than the hydrophobic layer, and the water absorption decreases.

Figure 5(a) shows the influence of different contents of lime, fly ash, and content on the saturation coefficient. With the increase of lime content, the saturation coefficient gradually increases. The reason is that with the increase of lime content, the porosity increases significantly and the water absorption increases, which is beneficial to the rapid test. Water absorption is saturated, so the saturation coefficient increases; with the increase of the fly ash content, the saturation coefficient gradually decreases. The reason is that with the increase of the fly ash content, the ability to improve the pore structure increases, and the large pores are gradually smaller. This causes the porosity to decrease, which is not conducive to the water saturation of the sample, so the saturation coefficient gradually decreases; as the cement content increases, the saturation coefficient gradually decreases. The reason is that the increase in cement content generates a large amount of C-S-H gel to wrap the sludge particles to fill the voids and make them denser, which is not conducive to testing. The sample is saturated with water, so the saturation coefficient increases. As shown in Figure 5(b), as the content of polyvinyl alcohol increases, the saturation coefficient increases slowly. When the content exceeds 1%, it decreases significantly. The reason is that when the content of polyvinyl alcohol is low, fewer hydrophobic layers are formed. It has little effect on 5 h and 24 h boiling samples. When the content exceeds 1%, the hydrophobic layer increases, and long-term boiling destroys the hydrophobic layer, and the water absorption increases, which significantly reduces the saturation coefficient.

3.3. Frost Resistance. Figure 6 shows the effect of different contents of polyvinyl alcohol on the compressive strength loss rate and mass loss rate of the sample after 15 freeze-thaw cycles. It can be seen from the figure that as the content of polyvinyl alcohol increases, the compressive strength loss rate and mass loss rate gradually decrease. When the polyvinyl alcohol content reaches 1%, the compressive strength loss rate and mass loss rate tend to be flat. Therefore, the addition of an appropriate amount of polyvinyl alcohol can improve frost resistance. When the content exceeds 1%, with the increase of polyvinyl alcohol, the frost resistance does not change significantly.

Figure 7 shows the appearance quality of the bricks before and after the freeze-thaw cycle. It can be seen from Figure 7(a) that before the freeze-thaw cycle, the surface of the brick is flat and smooth. However, it can be seen from Figure 7(b) that cracks and matrix flaking appear on the surface after the freeze-thaw cycle, which reduces the mechanical properties of the brick.

3.4. Porosity and Density. Figure 8(a) shows the influence of lime content on the pore size distribution and porosity. As the lime content increases, the porosity increases and the pore size gradually increases. The reason is that due to the increase of lime content, the reaction releases a lot of heat, and the generation of more $CaCO_3$ causes volume expansion, resulting in a large number of pores, even microcracks, and increasing porosity. As shown in Figures 8(b) and 8(d), with the increase of fly ash content, the porosity decreases, and the number of pores also decreases. The reason is that fly ash has a microaggregate effect. Due to the increase in fly ash content, the pore size is refined, the pore structure is improved, and the large pores are gradually smaller, resulting in a decrease in porosity. As shown in Figure 8(c), with the increase of cement content, the pore size, quantity, and porosity decreased, mainly due to the increase in cement content, which produced a large amount of C-S-H gel to wrap the sludge particles to fill the voids and make it denser. As shown in Figure 8(e), the pore size, number, and porosity increase significantly when polyvinyl alcohol is just added, and subsequently with the increase of polyvinyl alcohol, the pore size, number, and porosity increase slowly, because polyvinyl alcohol is a macromolecule. The presence of polymer blocks the link of C-S-H, and after polyvinyl alcohol is squeezed by the growing C-S-H, it is easy to form wrinkles, thereby increasing the porosity of the material. In addition, polyvinyl alcohol can adsorb $Ca(OH)_2$. As its content increases, the adsorptivity also increases, thereby filling part of the pores, and finally making the pores stable. Although the increase of polyvinyl alcohol increases the porosity, it refines the pore size and makes the pore size distribution more uniform.

Figure 9(a) shows the influence of different content of lime, fly ash, and cement on sample density. As the lime content increases, the density of the nonsintered sample gradually decreases. The reason is that with the increase of lime content, the porosity of the nonsintered brick increases, resulting in a decrease in density; when the lime content is 30%, as the proportion of fly ash increases, the density of the nonsintered brick sample gradually decreases. Although the porosity decreases, the decrease is small. The bulk density (approximately 0.8 g/cm^3) is much lower than that of the muck soil (approximately 1.4 g/cm^3). The influence of low fly ash density is much greater than the influence of porosity on density. Therefore, as the content of fly ash increases, density

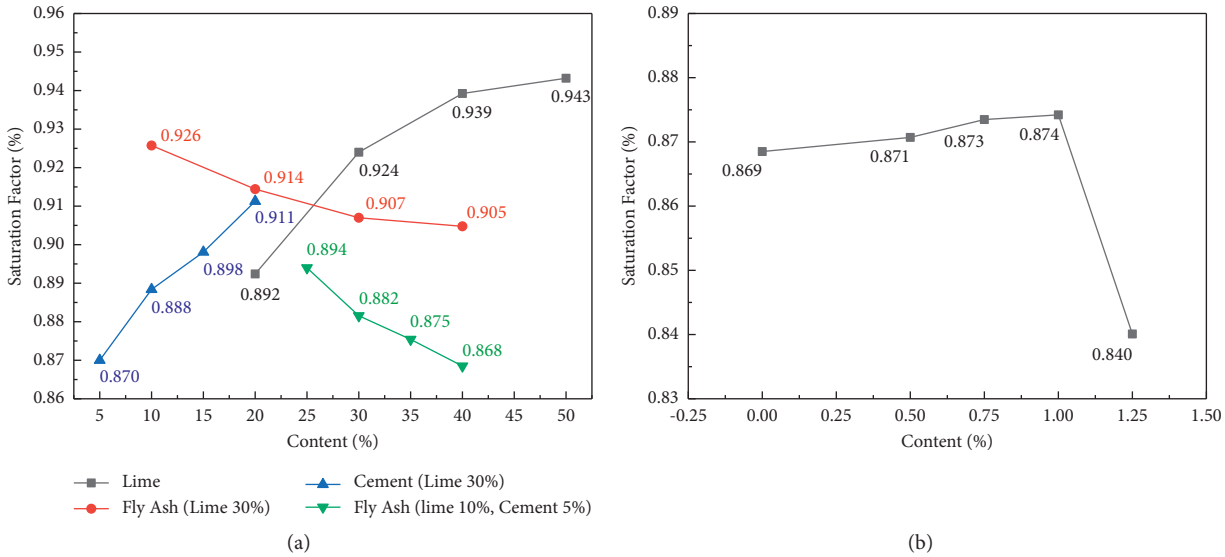

Figure 5: The influence of lime, fly ash, cement (a), and polyvinyl alcohol (lime 10%, cement 5%, and fly ash 40%) (b) on saturation coefficient.

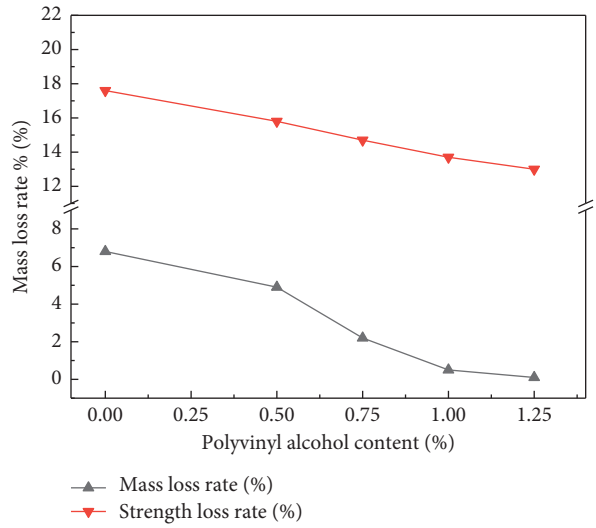

Figure 6: The loss rate of quality and tensile strength after 15 freeze-thaw cycles.

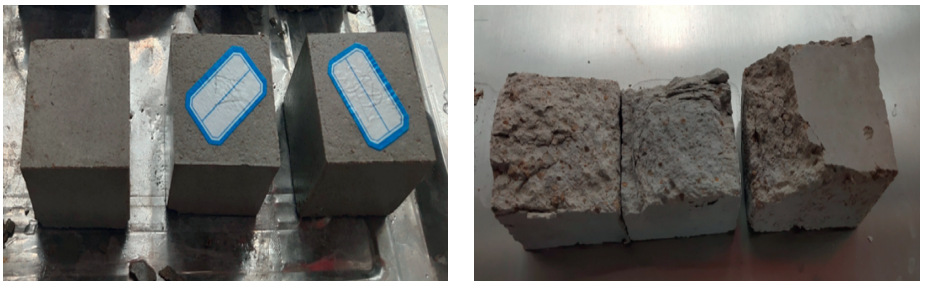

Figure 7: The sample photos before (a) and after (b) freeze-thaw test.

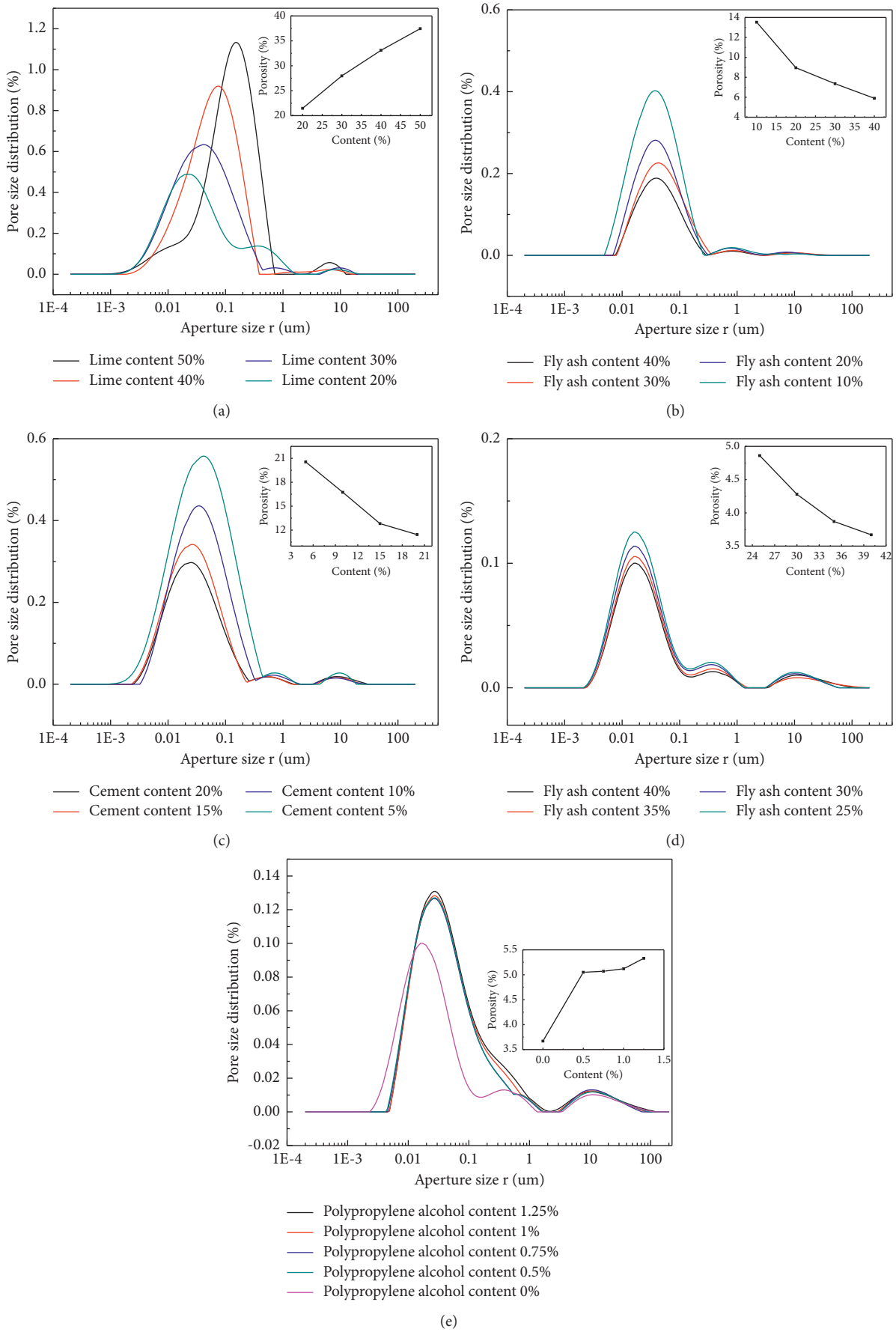

Figure 8: The influence of different content of lime (a), fly ash (lime 30%) (b), cement (lime 30%) (c), fly ash (lime 10%, cement 5%) (d), and polyvinyl alcohol (lime 10%, cement 5%, fly ash 40%) (e) on the pore size distribution and porosity.

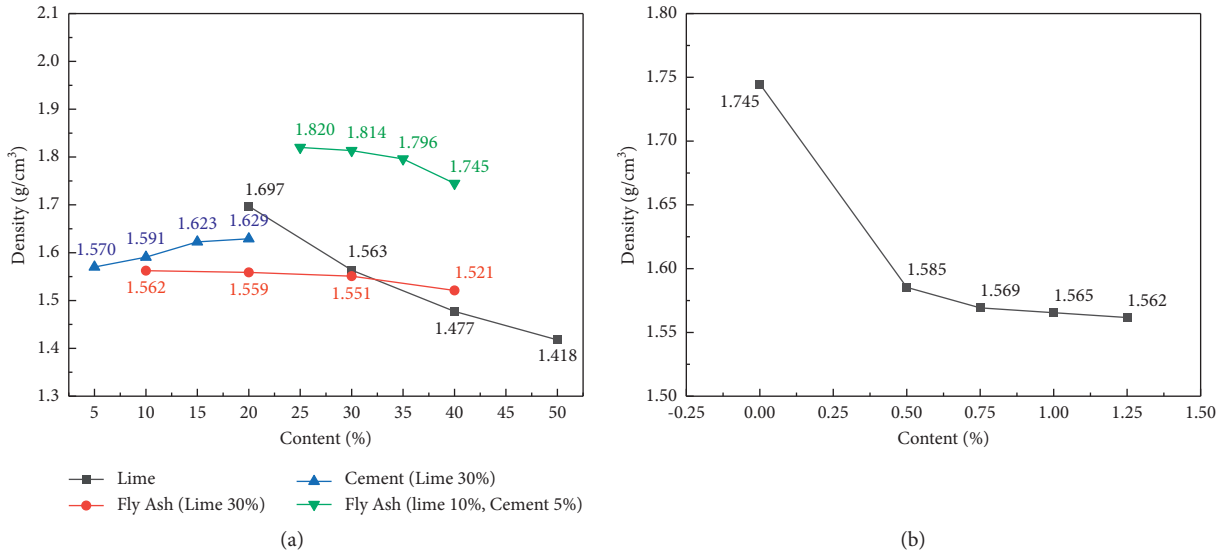

Figure 9: The influence of different content of lime, fly ash, cement, and polyvinyl alcohol (lime 10%, cement 5%, and fly ash 40%) on sample density.

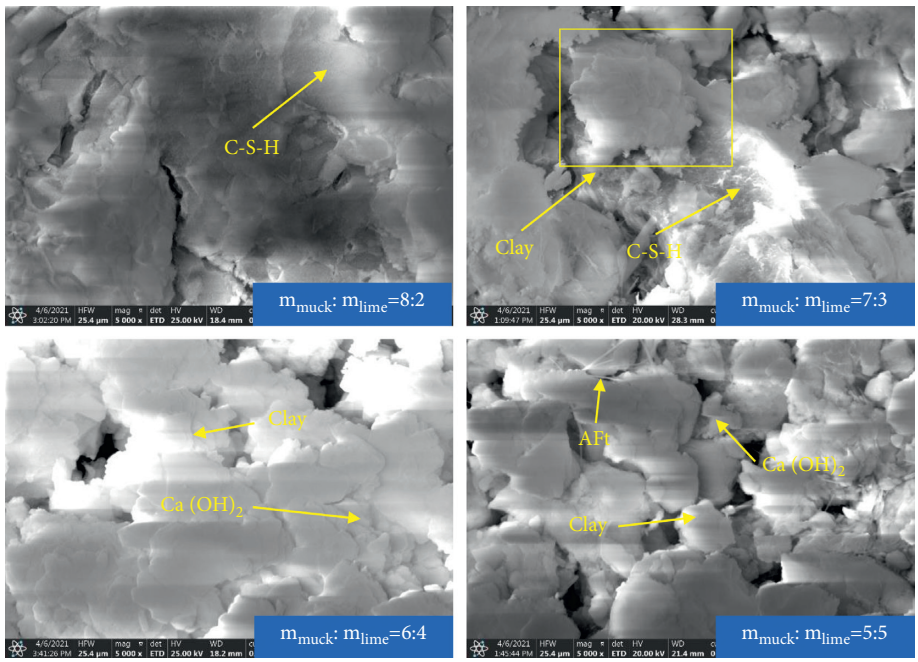

Figure 10: SEM images of nonsintered bricks with different lime doping levels.

is reduced; when the lime content is 30%, as the cement content increases, the porosity of the nonsintered brick sample decreases and the density increases; when the lime content is 10% and the cement content is 5%; as the fly ash content increases, the density also shows a downward trend. As shown in Figure 9(b), when the lime content is 10% and the cement content is 5%, the doping of polyvinyl alcohol can significantly reduce the density of the nonsintered brick samples. With the increase of the doping amount, the density gradually decreases. The reason is that the addition of polyvinyl alcohol instantly increases the porosity of the nonsintered bricks, resulting in a significant decrease in density. With the increase in the amount of addition, the porosity of the nonsintered bricks increases gently, resulting in a gentle decrease in density.

3.5. Microstructure. Figure 10 shows SEM images of nonsintered bricks with different lime contents. With the increase of lime content, the morphology of nonsintered bricks gradually changes from compactness to looseness, and the bulk silicate and tabular $Ca(OH)_2$ gradually increase, and the

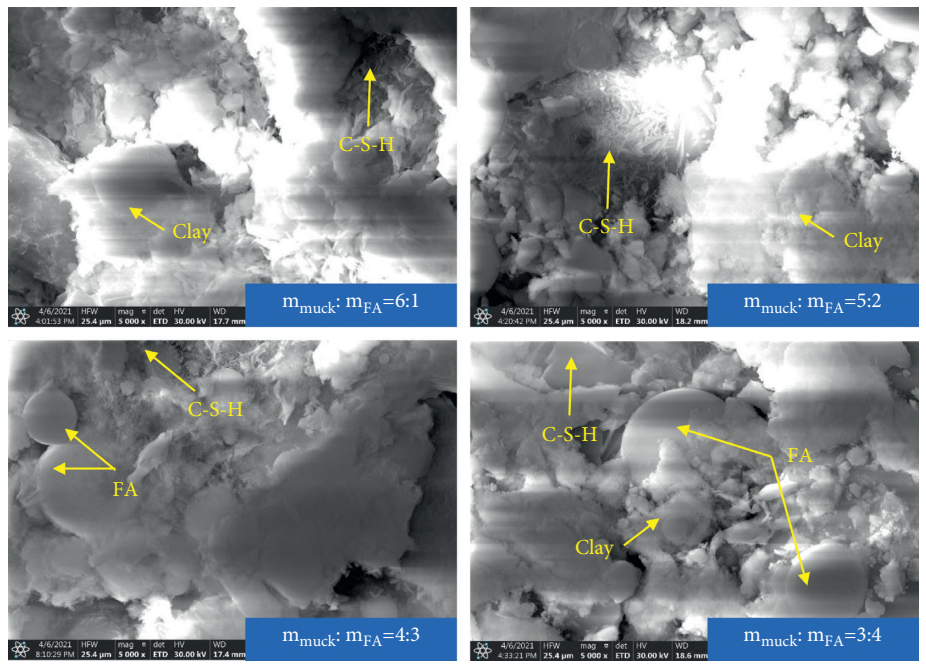

Figure 11: SEM images of nonsintered bricks with different fly ash content.

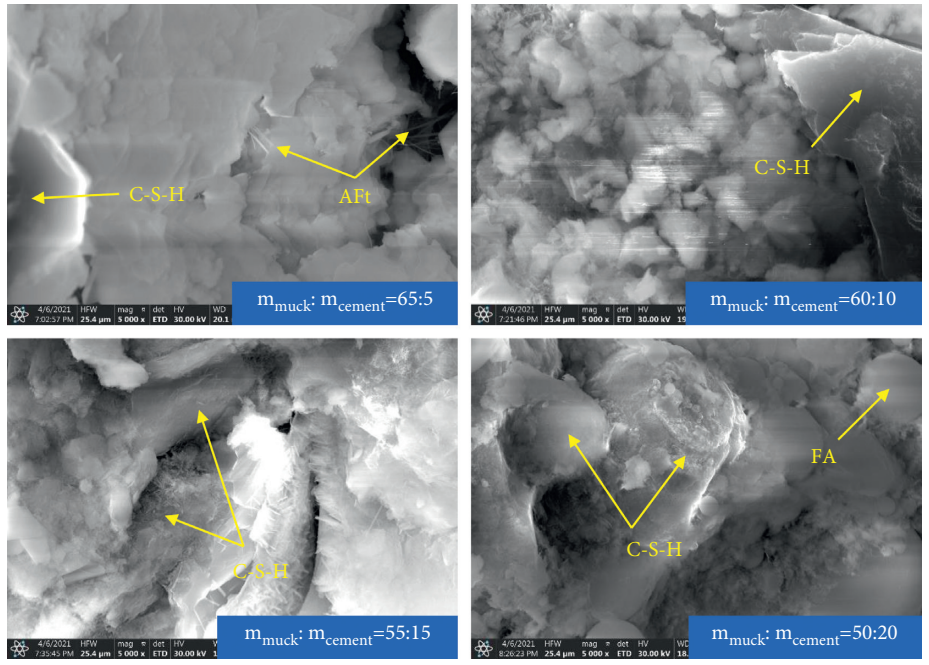

Figure 12: SEM images of nonsintered bricks with different cement content.

porosity increases. When the calcium oxide content is too high, the hydrated silicate minerals are filled and connected by nonbonding $Ca(OH)_2$ through the pores between them, so that the overall structure becomes loose. This explains that in the absence of cement and fly ash, the strength of the specimen decreases with the increase of the amount of lime, indicating that in the preparation of slag soil fired brick, adding a small amount of lime to make the whole gel system in an alkaline environment can stimulate the activity of clay minerals, and the increase of CaO will adversely affect the integrity of the system, thus reducing the strength of the system.

Figure 11 shows SEM images of nonsintered bricks with different fly ash doping contents (lime 30%). Due to the addition of lime, the system is a strong alkali system, and the activity of fly ash is quickly activated to form a large amount of C-S-H, thus ensuring the integrity of the system. The activity of fly ash is much higher than that of unsintered slag

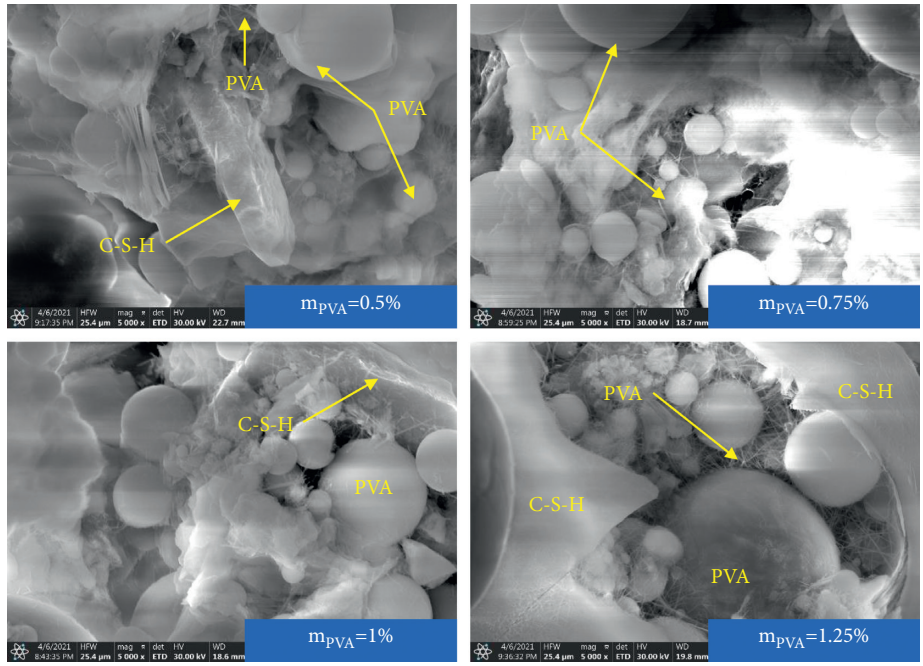

Figure 13: SEM images of nonsintered bricks with different polyvinyl alcohol doping levels (muck 45%, lime 10%, cement 5%, and fly ash 40%).

soil. The content of C-S-H increases continuously, and the compactness of the system increases continuously, thus increasing the strength of the system.

Figure 12 shows SEM images of nonsintered bricks with different cement content. The addition of cement will significantly enhance the activity of the whole system, C-S-H will significantly increase, and the integrity of the system will be stronger. With the increase of cement content, the surface particles will gradually decrease, and the overall compactness will be better, and the strength of the specimen will be significantly enhanced.

Figure 13 shows SEM images of nonsintered bricks with different polyvinyl alcohol content. The addition of polyvinyl alcohol makes the three-dimensional network structure formed between the cementitious materials. With the increase of polyvinyl alcohol, the alcoholysis ratio decreases, and the unalcoholized polyvinyl alcohol forms spherical particles, which are distributed in the cementitious materials; as a result, the compactness of the gel was reduced, and polyvinyl alcohol particles filled the pores of the system and reduced the porosity of the system. However, polyvinyl alcohol did not have gelation, resulting in the increase of polyvinyl alcohol in the pores and the decrease in the strength of the system. In addition, when polyvinyl alcohol was added, the C-S-H surface was smoother, the water resistance was enhanced, and the elastic effect of spherical vinyl alcohol would increase the toughness and frost resistance of the material.

4. Conclusion

Based on shield slag, the fire-free bricks were successfully prepared. By mixing different proportions of lime, fly ash, cement, and polyvinyl alcohol, the effects of porosity, density, water absorption, saturation coefficient, microscopic morphology, and mechanical properties were explored. The law of influence is as follows:

(1) With the increase of lime content, the porosity increases, the density decreases, the water absorption and saturation coefficient increase, and the compressive strength first decreases. Therefore, lime is not suitable for being added in large quantities during the preparation process of nonsintered bricks.

(2) When the lime content is 30%, with the increase of the fly ash and cement content, the porosity, density, water absorption, and saturation coefficient will decrease at the same time, and the compressive strength will increase. But the effect of fly ash on the properties of test blocks is not as obvious as cement. After cement and fly ash are mixed, porosity and a density decrease, water absorption increases, saturation coefficient decreases, and compressive strength increase significantly with the increase of fly ash doping amount.

(3) With the increase of the doping amount of polyvinyl alcohol, porosity increases, density decreases, water absorption, and saturation coefficient increase first and then decrease, and the strength of the specimen decreases significantly, but the pure toughness of polyvinyl alcohol significantly enhances the freezing resistance of the specimen.

(4) The research in this paper provides a new way for the reuse of shield tunnel muck. When the muck is mixed with 45%, lime 10%, cement 5%, and fly ash 40%, the strength can reach 13.69 MPa, reaching the

standard strength level. MU10 meets engineering applications, such as non-load-bearing walls and roadbed pavement paving. The resource utilization of shield dregs is realized, the ecological environment is protected, and the amount of cement is reduced at the same time, which has significant economic benefits.

Data Availability

All data included in this study are available upon request by contact with the corresponding author.

Disclosure

The views expressed here were the authors' alone.

Conflicts of Interest

The authors declare that there are no conflicts of interest regarding the publication of this study.

Acknowledgments

Throughout the writing of this dissertation, we have received a great deal of support and assistance. This article was funded by Science and Technology Program of the Ministry of Housing and Urban-Rural Development (no. 2020-K-142), Shandong Province Housing and Urban-Rural Construction Science and Technology Plan Project (no. 2019-S7-1), Shandong Provincial Key Research and Development Program (no. 2019JZZY010428), and National Natural Science Foundation of China (no. 51809158 and no. 51909143). Thanks are due to our tutors and classmates for their patience and excellent cooperation.

References

[1] P. Marini and R. Bellopede, "The use of tunnel muck as industrial raw material: two case-studies," *Rock Mechanics and Rock Engineering*, vol. 46, no. 2, pp. 397–404, 2013.

[2] C. Oggeri, T. M. Fenoglio, and R. Vinai, "Tunnel spoil classification and applicability of lime addition in weak formations for muck reuse," *Tunnelling and Underground Space Technology*, vol. 44, pp. 97–107, 2014.

[3] X. Li, Q. Huang, P. Wang, D. Huang, and F. Geng, "Back-fill grouting and proper performance for discharged soils reuse of the slurry shield tunnel on sand stratum," *Journal of Building Materials*, vol. 22, no. 2, pp. 299–307, 2019.

[4] S. W. Tang, Y. Wang, Z. C. Geng, X. F. Xu, and W. Z. Yu, "Structure, fractality, mechanics and durability of calcium silicate hydrates," *Fractal and Fractional*, vol. 5, no. 2, p. 47, 2021.

[5] R. J. Liu, Q. J. Ding, P. Chen, and G. Y. Yang, "Durability of concrete made with manganese slag as supplementary cementitious materials," *Journal of Shanghai Jiaotong University*, vol. 17, no. 3, 2012.

[6] X. Y. Guo, Z. D. Chen, L. Z. Pei, J. M. Li, and C. G. Fan, "Preparation and characterization of sintering-free bricks based on modified slag cement & muck," *New Building Materials*, vol. 47, no. 5, pp. 75–79, 2020.

[7] L. Wang, F. X. Guo, Y. Q. Lin, H. M. Yang, and S. W. Tang, "Comparison between the effects of phosphorous slag and fly ash on the C-S-H structure, long-term hydration heat and volume deformation of cement-based materials," *Construction and Building Materials*, vol. 250, Article ID 118807, 2020.

[8] K. Ehsan and T. Vahab, "Reliability analysis of rammed earth structures," *Construction and Building Materials*, vol. 127, pp. 884–895, 2016.

[9] X. Qian, C. Guan, Y. Y. Chen, F. L. Ling, and S. Y. Wang, "Experimental study on reusing soil dug by EPB shield from clay layer to synchronous grouting," *Hazard Control in Tunnelling and Underground Engineering*, vol. 2, no. 1, pp. 68–74, 2020.

[10] Y. Cui and Z. Tan, "Experimental study of high performance synchronous grouting materials prepared with clay," *Materials*, vol. 14, no. 6, p. 1362, 2021.

[11] L. Zhang, H. F. Zhang, H. Rong, and J. J. Yang, "Fabrication and performance of 700900 density grade muck ceramsite(article)," *Jianzhu Cailiao Xuebao/Journal of Building Materials*, vol. 21, no. 5, pp. 803–810, 2018.

[12] W. Yang, Y. X. Chen, H. C. Wang, X. L. Lei, and Z. Zeng, "Study on the preparation technology of chromium contaminated soil-fly ash ceramsite," *Journal of Functional Materials/Gongneng Cailiao*, vol. 49, no. 9, pp. 09169–09179, 2018.

[13] W. Yao, J. Pang, and Y. Liu, "Performance degradation and microscopic analysis of lightweight aggregate concrete after exposure to high temperature," *Materials*, vol. 13, no. 7, p. 1566, 2020.

[14] S. Liu, C. G. Yang, W. Liu, L. S. Yi, and W. Q. Qin, "A novel approach to preparing ultra-lightweight ceramsite with a large amount of fly ash," *Frontiers of Environmental Science & Engineering*, vol. 14, no. 4, pp. 74–84, 2020.

[15] L. Wang, R. Y. Luo, W. Zhang, M. M. Jin, and S. W. Tang, "Effects of fineness and content of phosphorus slag on cement hydration, permeability, pore structure and fractal dimension of concrete," *Fractals*, vol. 29, no. 2, Article ID 2140004, 2021.

[16] J. H. Xie, J. B. Zhao, J. J. Wang, P. Y. Huang, and J. F. Liu, "Investigation of the high-temperature resistance of sludge ceramsite concrete with recycled fine aggregates and GGBS and its application in hollow blocks," *Journal of Building Engineering*, vol. 34, Article ID 101954, 2020.

[17] E. Sandra, O. Joshua, M. Sara, E. Angel Maria, and S. Andres, "Magnesium oxide as alternative binder for unfired clay bricks manufacturing," *Applied Clay Science*, vol. 146, pp. 23–26, 2017.

[18] A. Seco, J. Omer, S. Marcelino, S. Espuelas, and E. Prieto, "Sustainable unfired bricks manufacturing from construction and demolition wastes," *Construction and Building Materials*, vol. 167, pp. 154–165, 2018.

[19] M. N. Rahmat, N. Ismail, and K. John Mungai, "Strength and environmental evaluation of stabilised Clay-PFA eco-friendly bricks," *Construction and Building Materials*, vol. 125, pp. 964–973, 2016.

[20] F. Abd-El-Raoof, A. Tawfik, and H. M. Abdelaal, "Two-stage sintering of eco-friendly chromium-free bricks from available wastes," *Interceram - International Ceramic Review*, vol. 69, no. 2, pp. 38–45, 2020.

[21] L. Wang, M. Jin, S. Zhou, S. W. Tang, and X. Lu, "Investigation of microstructure of C-S-H and micro-mechanics of cement pastes under NH4NO3 dissolution by 29Si MAS NMR and microhardness," *Measurement*, vol. 185, Article ID 110019, 2021.

[22] S. Sumi and P. N. M. Barreto, "Chemical stabilization of rammed earth using calcium carbide residue and fly ash," *Construction and Building Materials*, vol. 169, pp. 364–371, 2018.

[23] S. Q. Sun, P. He, G. Wang et al., "Shape characterization methods of irregular cavity using Fourier analysis in tunnel," *Mathematics and Computers in Simulation*, vol. 187, pp. 191–214, 2021.

[24] L. Wang, M. M. Jin, F. X. Guo, Y. Wang, and S. W. Tang, "Pore structural and fractal analysis of the influence of fly ash and silica fume on the mechanical property and abrasion resistance of concrete," *Fractals*, vol. 29, no. 2, Article ID 2140003, 2021.

[25] Y. Zhang, S. Wang, B. Zhang, D. Hou, H. Li, and L Li, "A preliminary investigation of the properties of potassium magnesium phosphate cement-based grouts mixed with fly ash, water glass and bentonite," *Construction and Building Materials*, vol. 23, 2020.

[26] A. J. Boyd and A. Leone, "Effect of freeze-thaw cycling on fatigue behaviour in concrete," *IOP Conference Series: Materials Science and Engineering*, vol. 652, no. 1, Article ID 012028, 2019.

[27] O. Gencel, M. J. Munir, S. M. S. Kazmi et al., "Recycling industrial slags in production of fired clay bricks for sustainable manufacturing," *Ceramics International*, vol. 47, no. 21, pp. 30425–30438, 2021.

[28] *GB/T 2542-2012*, Test Method for Wall Bricks, China, 2012.